Visualizing Phase Transition Behavior of Dilute Stimuli Responsive Polymer Solutions via Mueller Matrix Polarimetry

ARTICLE *in* ANALYTICAL CHEMISTRY · AUGUST 2015

Impact Factor: 5.64 · DOI: 10.1021/acs.analchem.5b01794 · Source: PubMed

4 AUTHORS, INCLUDING:

Amal Narayanan

University of Akron

5 PUBLICATIONS **9** CITATIONS

SEE PROFILE

Shubham Chandel

Indian Institute of Science Education and Res…

11 PUBLICATIONS **11** CITATIONS

SEE PROFILE

analytical chemistry

Technical Note

pubs.acs.org/ac

Visualizing Phase Transition Behavior of Dilute Stimuli Responsive Polymer Solutions via Mueller Matrix Polarimetry

Amal Narayanan,[†] Shubham Chandel,[‡] Nirmalya Ghosh,*[,‡] and Priyadarsi De*[,†]

[†]Polymer Research Centre, Department of Chemical Sciences, [‡]Department of Physical Sciences, Indian Institute of Science Education and Research Kolkata, Mohanpur 741246, Nadia, West Bengal, India

Supporting Information

ABSTRACT: Probing volume phase transition behavior of superdiluted polymer solutions both micro- and macroscopically still persists as an outstanding challenge. In this regard, we have explored 4 × 4 spectral Mueller matrix measurement and its *inverse* analysis for excavating the microarchitectural facts about stimuli responsiveness of "*smart*" polymers. Phase separation behavior of thermoresponsive poly(*N*-isopropylacrylamide) (PNIPAM) and pH responsive poly(*N*,*N*-(dimethylamino)ethyl methacrylate) (PDMAEMA) and their copolymers were analyzed in terms of Mueller matrix derived polarization parameters, namely, depolarization (Δ), diattenuation (*d*), and linear retardance (*δ*). The Δ, *d*, and *δ* parameters provided useful information on both macro- and microstructural alterations during the phase separation. Additionally, the two step action ((i) breakage of polymer−water hydrogen bonding and (ii) polymer−polymer aggregation) at the molecular microenvironment during the cloud point generation was successfully probed via these parameters. It is demonstrated that, in comparison to the present techniques available for assessing the hydrophobic−hydrophilic switch over of simple stimuli-responsive polymers, Mueller matrix polarimetry offers an important advantage requiring a few hundred times dilute polymer solution (0.01 mg/mL, 1.1−1.4 μM) at a low-volume format.

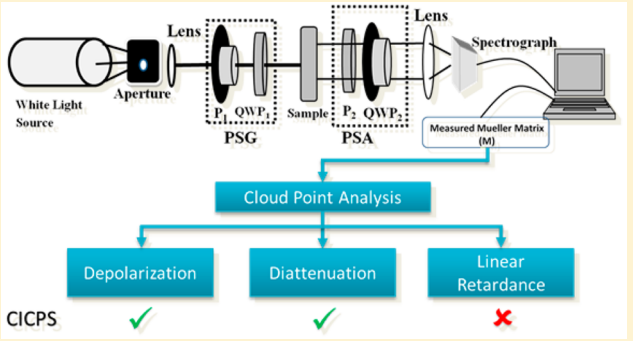

Stimuli-responsive or "*smart*" polymers can undergo volume phase transition in response to physiochemical changes in the microenvironment, viz., temperature, pH, light, enzyme, etc.[1] Though visualization of this phase separation behavior microscopically remains to be a challenge, the past few decades witnessed prolific progression in the field of stimuli-responsive polymers (SRPs).[2] The relevance of such smart systems in nanotechnology for tissue engineering,[3] biosensors,[4] protein purification,[5−7] controlled drug delivery,[8] catalysis,[9] smart surfaces,[10] etc. is well-investigated in due course. The specific stimuli responsiveness arises either from switching in equation of state effects (EOS) or from the disruption of strong directional interactions such as hydrogen bonding by external stimuli.[11] To determine the effective phase separation point (cloud point), experimental techniques like ^{1}H NMR spectroscopy, differential scanning calorimetry (thermodynamic contributions), viscosity measurements (hydrodynamic parameters), light scattering (molecular size change), UV−visible spectroscopy (molecular macroscopic phase behavior), etc. have been employed.[12,13] Among previously listed methodologies, the transmittance measurement through UV−visible spectroscopy is well established and extensively utilized.[14] The major disadvantage of this quantification method is the requirement of highly concentrated polymer solutions (∼1−10 mg/mL) for cloud point analysis.[15] The above-mentioned drawback restricts the applicability of UV−visible spectroscopy in evaluating the exquisite properties of "*smart*" polymers while framing bioconjugates and nano-objects. In this context, Nash and co-workers reported the analysis of thermoresponsiveness behavior of BODIPY labeled oligo(ethylene glycol) (OEG) methyl ether methacrylate copolymer through thermophoretic measurements at nanomolar level polymer concentration.[16] Unfortunately, this method requires polymers labeled with a dye for phase transition quantifications; hence, the approach lacks a general appeal. To the best of our knowledge, there is no single technique developed, which permits determination of cloud points of polymers without any chemical modification at the concentration range of <0.10 mg/mL.

The Mueller matrix, a 4 × 4 matrix, describes the transfer function of any medium in its interaction with polarized light and encodes information on all the intrinsic sample polarization properties in its various elements.[17] The *inverse* analysis method with polar decomposition provides an opportunity to scrutinize the intrinsic sample polarization properties of any medium in terms of linear retardance (*δ*), diattenuation (*d*), and depolarization (Δ) parameters.[18] These parameters when individually separated and analyzed can provide immense qualitative as well as quantitative microscopic, functional, and orientational/organizational information. For example, Patil et

Received: May 13, 2015
Accepted: August 19, 2015

DOI: 10.1021/acs.analchem.5b01794
Anal. Chem. XXXX, XXX, XXX−XXX

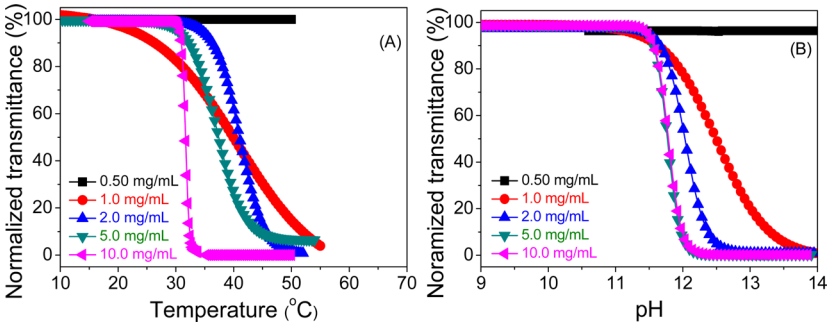

Figure 1. (A) Temperature dependent transmittance of PNIPAM and (B) pH dependent transmittance of PDMAEMA at 500 nm.

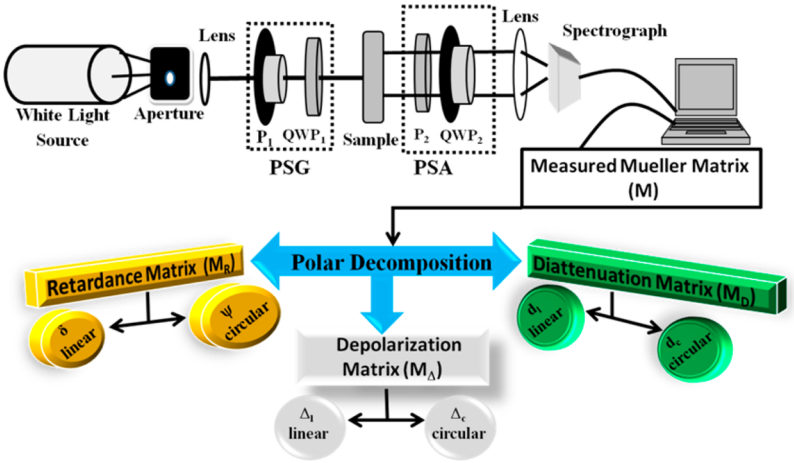

Figure 2. Schematics of the experimental MMP system and its *inverse* analysis using the polar decomposition method. P1 and P2 are linear polarizers, and QWP_1 and QWP_2 are sequentially changed to set its position for the generation of optimized polarization state.

al. have described the ability of Mueller matrix polarimetry (MMP) to study structural information and macroscopic deswelling kinetics of covalently cross-linked[19] and cadmium sulfide quantum dots doped nanocomposite hydrogels.[20] Even though the experimental measures for MMP are sophisticated, a study for improving the time scale required to enable MMP for quantifying dynamic processes was reported recently.[21]

Among the wide class of SRPs, the most exploited phase separation behavior is the aqueous solution property of poly(*N*-isopropylacrylamide) (PNIPAM) and poly(*N*,*N*-(dimethylamino)ethyl methacrylate) (PDMAEMA). Both the polymeric systems show lower critical solution temperature (LCST) in water, and interestingly, PDMAEMA has responsiveness toward pH as well. In the present study, we have established a novel method for investigating both micro- and macroscopic events occurring during the phenomena of phase separation by homopolymers (PNIPAM and PDMAEMA) and their copolymers poly(*N*-isopropylacrylamide-*co*-*N*,*N*-dimethylacrylamide) [PNIPAM-*co*-DMA] and poly(*N*,*N*-(dimethylamino)ethyl methacrylate-*co*-methyl methacrylate) [P(DMAEMA-*co*-MMA)] via the Mueller matrix derived δ, d, and Δ polarization parameters.

EXPERIMENTAL SECTION

Synthesis of Polymers. The polymers with number-average molecular weight (M_n) = 7000−12 000 g/mol were synthesized through reversible addition−fragmentation chain transfer (RAFT) polymerization (Scheme S1)[22] to obtain polymers with narrow molecular weight distribution ($Đ$).[23] The details regarding polymerization conditions and characterizations are summarized in Table S1.

Analysis via UV−vis Spectroscopy. Initially, phase transition points of the polymers were determined through pH/temperature dependent transmittance measurement at 500 nm by UV−visible spectroscopy.[24] The point at which 50% transmittance drop occurred was assigned as the cloud point of the polymer.[25] The transmittance measurement derived cloud points (Figures 1 and S1) were in accordance with the previously reported values.[22] 1.0 mg/mL was the minimum concentration at which cloud point measurement through transmittance was possible; below this particular concentration, the stimuli dependent transmittance curve did not show any appreciable slope even at extreme changes exerted by external stimuli. We observed a concentration induced cloud point shift (CICPS), which after a specific concentration leveled off, as described elsewhere.[26] Various groups have studied the effect of cloud point on polymer concentration, and cloud point is often mistakenly interpreted as LCST. The higher dependency of cloud point on polymer concentration has been a major motivation for the replacement of PNIPAM by poly[2-(2-methoxyethoxy)ethyl methacrylate-*co*-oligo(ethylene glycol) methacrylate] and substituted poly(2-oxazoline)s in recent years.[26] Rather than CICPS, we observed an increment in the slope of sigmoidal curve at higher polymer concentration. This trend may arise due to the quicker intra/inter polymer interactions plausible at higher polymer concentration. The phenomenon of cloud point generation is governed by two events: (i) the disruption of water−polymer hydration shell by external stimuli followed by water expulsion and (ii) the

DOI: 10.1021/acs.analchem.5b01794
Anal. Chem. XXXX, XXX, XXX−XXX

increment in solution turbidity originating from polymer−polymer aggregation.[27] It is understood that the proximity of polymer molecules will accelerate the second event. The entire event of this phase separation is related to the coil to globule transition (CGT), which is explained using the lattice fluid model and scaled particle theory.[28] The UV−visible spectroscopy allowed us to only probe the turbidity of the medium which is a bulk property, not necessarily the microscopic phase transition point.

Experimental Mueller Matrix Setup. The experimental system is comprised of a white light source (xenon lamp) for elastic scattering spectral measurement, collimating optics, polarization state generator (PSG) unit, sample chamber, polarization state analyzer (PSA) unit, and a spectrograph for the spectrally resolved signal detection.[29] The PSG unit consists of a fixed linear polarizer P1 with its axis aligned along the horizontal direction and a computer controlled rotating achromatic quarter wave plate (QWP_1) as a combination to generate the four required (and optimized) elliptical polarization states. PSA is just the same system placed in reverse order (with the axis of the linear polarizer P2 fixed along the vertical direction and the quarter wave plate QWP_2 sequentially oriented to the same angles as PSG) to analyze these four elliptical states. In order to generate the four optimized elliptical polarization states, the axis of quarter wave plate was sequentially changed to set its position to 35°, 70°, 105°, and 140° with respect to the polarizer axis. The light scattered (and transmitted) from the sample is collected and collimated using an assembly of lenses, then passed through the PSA unit, and finally recorded using a spectrometer (Figure 2). The 4 × 4 spectral Mueller matrices were constructed using the 16 measurements performed with the combination of PSG and PSA. During the measurements, s few microliters (∼5−10) of polymer solution was transferred to a cuvette with 0.1 cm breadth, 2.0 cm depth, and 1.0 cm path length. The wavelength range of 550 to 700 nm was kept as the working range for the polarimetry measurements in which the polymers exhibited negligible absorption.[19]

Stokes Mueller Matrix Algebra. For each optimized angle of QWP_1 in PSG, an elliptical polarized state is generated and sequentially analyzed by PSA unit. The four set of Stokes vector, when written in column format, forms a 4 × 4 matrix **W** (representing the PSG unit), whereas when written in row format, forms a 4 × 4 matrix **A** (PSA unit). The 16 recorded intensity measurements are grouped in a 4 × 4 matrix $\mathbf{M_i}$, which is related to the **A** and **W** matrix as $\mathbf{M_i} = \mathbf{A}\cdot\mathbf{M_s}\cdot\mathbf{W}$, where $\mathbf{M_s}$ is the sample Mueller matrix. Once the exact experimental form of **A** and **W** is known, the sample Mueller matrix can be calculated as

$$\mathbf{M_s} = A^{-1}\cdot\mathbf{M_i}\cdot\mathbf{W}^{-1}$$

The spectral Mueller matrix was thus determined for the wavelength range of 550−700 nm with spectral resolution of 2.0 nm. The exact nature of these **W** and **A** matrices are determined using the so-called Eigen Value Calibration (ECM) method. It compensates for the wavelength dependence, nonideal behavior of optical components, misalignments, and etc. as explained elsewhere.[30]

***Inverse* Analysis Based on Mueller Matrix Decomposition.** We now briefly introduce the concept of Mueller matrix and its *inverse* analysis. The polarization state of light is presented by four measurable quantities known as Stokes vector grouped in a 4 × 1 vector (*I*, *Q*, *U*, *V* are the elements of the Stokes vector **S**). While the Stokes vector engraves the polarization properties of light, the Mueller matrix contains complete information about all the polarization properties of the interacting medium. The 4 × 4 Mueller matrix is a mathematical description of the polarization altering interaction of light with a medium exhibiting intrinsic polarimetry characteristics,

$$\mathbf{S_o} = \mathbf{M}\mathbf{S_i}$$

where $\mathbf{S_i}$ and $\mathbf{S_o}$ are the input and the output Stokes vectors, respectively. Various schemes have been developed to record a 4 × 4 Mueller matrix of any medium. As discussed above, we have utilized an in-house developed automated spectral 4 × 4 Mueller Matrix measurement system[30] (Figure 2), to record the full spectral Mueller matrix from the polymer solutions. The three basic polarization properties that are encoded in the various elements of Mueller matrix are diattenuation, retardance, and depolarization. Diattenuation is defined as differential attenuation of orthogonal linear polarizations (between horizontal and vertical or between +45° and −45°, accordingly termed as linear diattenuation) and orthogonal circular polarizations (between left and right, circular diattenuation). Retardance property on the other hand, deals with phase shifts between orthogonal linear polarizations (linear retardance) and circular polarizations (circular retardance or optical rotation). The third polarization property, depolarization, refers to loss of polarization due to randomization in polarization (e.g, by multiple scattering events). For samples exhibiting multiple polarization effects that are also in the presence of scattering (as is the case for the samples studied here), the recorded Mueller matrix represent "*lumped*" effects resulting in inter element cross talk, masking potentially interesting intrinsic polarization metrics. In order to extract and quantify the constituent polarimetry effects, the recorded Mueller matrix was then decomposed using the polar decomposition technique. Using this approach, the recorded Mueller matrix of any complex system is decomposed as the product of three basis matrices:

$$\mathbf{M} \Leftarrow \mathbf{M_\Delta}\cdot\mathbf{M_R}\cdot\mathbf{M_D}$$

Here, the matrix $\mathbf{M_R}$ contains the retardance effect (both circular and linear), $\mathbf{M_D}$ expresses the effect of linear and circular diattenuation, and $\mathbf{M_\Delta}$ describes the depolarizing effects of the medium. This decomposition technique was proposed by Lu and Chipman[18] at first, and very recently, it has been extended to extract polarization information from turbid media.[31] From the decomposed matrices, the relevant polarization parameters are quantified as

$$\Delta = 1 - \frac{|Tr(\mathbf{M_\Delta}) - 1|}{3}$$

$$D = \frac{1}{\mathbf{M_D}(1,1)}\sqrt{\mathbf{M_D}(1,2)^2 + \mathbf{M_D}(1,3)^2 + \mathbf{M_D}(1,4)^2}$$

$$\delta = \cos^{-1}\left\{\sqrt{[\mathbf{M_R}(2,2) + \mathbf{M_R}(3,3)]^2 + [\mathbf{M_R}(3,2) - \mathbf{M_R}(2,3)]^2} - 1\right\}$$

RESULTS AND DISCUSSION

In order to explore the possibility of probing the cloud point of homo- and copolymers, the recorded spectral Mueller matrices from PDMAEMA (for example) at two different conditions are

DOI: 10.1021/acs.analchem.5b01794
Anal. Chem. XXXX, XXX, XXX−XXX

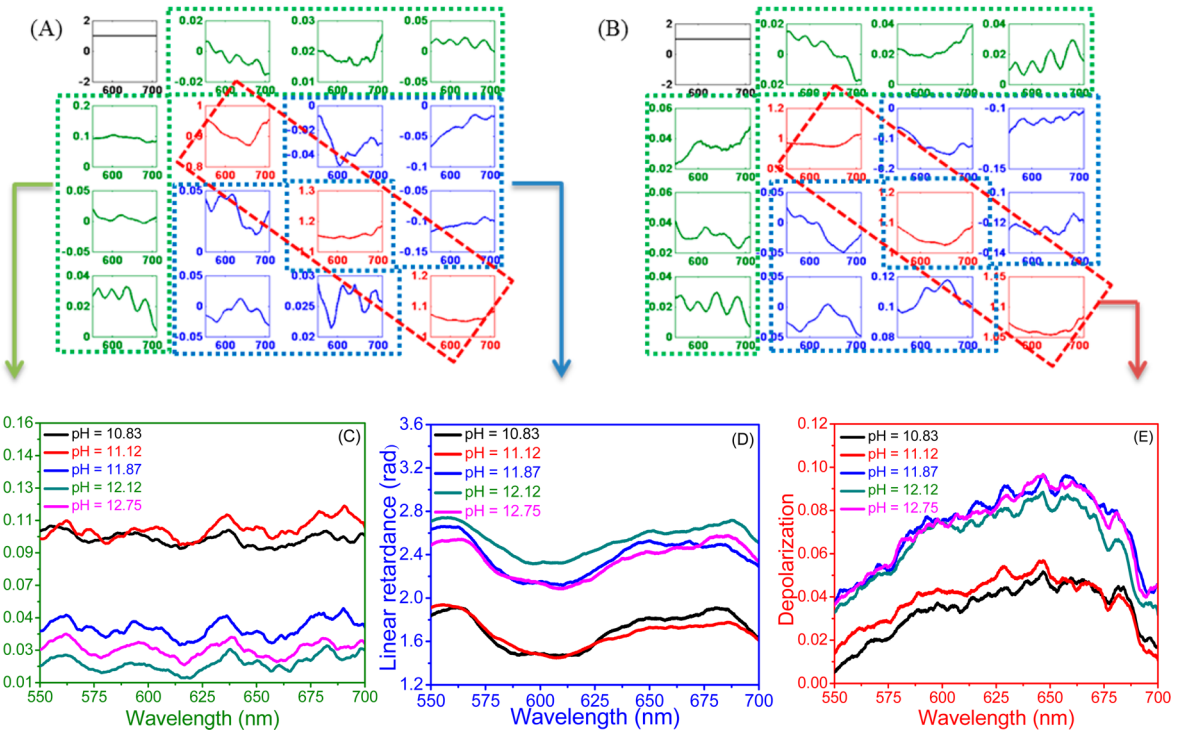

Figure 3. pH dependent recorded Mueller matrix (A) before and (B) after phase transition pH and the decomposed parameters (C) diattenuation, (D) linear retardance, and (E) depolarization of PDMAEMA solution at 25 °C.

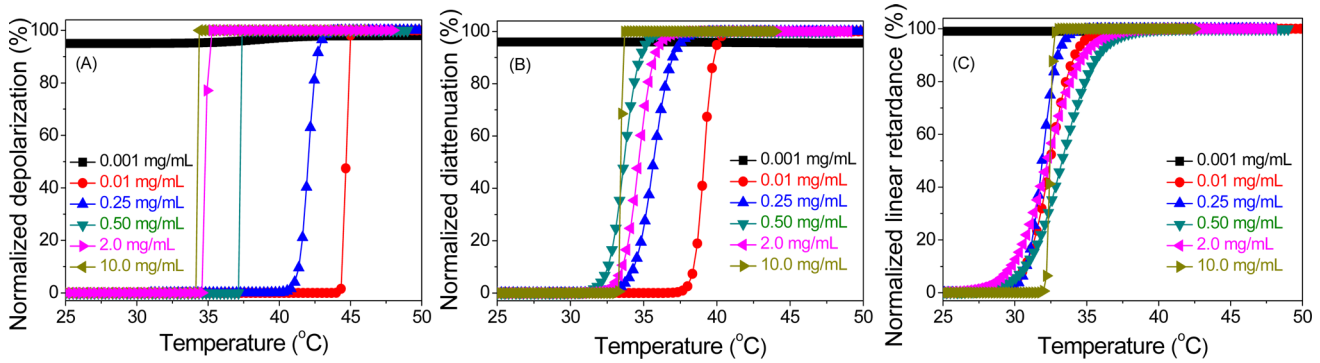

Figure 4. Temperature dependent (A) depolarization, (B) diattenuation, and (C) linear retardance of PNIPAM at 600 nm.

shown in Figure 3. The M_{11} element of a Mueller Matrix represents the total intensity. In this case, the matrix is normalized with M_{11} element. The diagonal elements (shown with red dots) primarily reflect the depolarization effect which is the loss of polarization due to multiple scattering and random orientations. The higher values of diagonal elements are attributed to lesser loss of polarization corresponding to reduced multiple scattering or turbidity at lower pH. The elements M_{24}, M_{42}, M_{34}, and M_{43} (shown with blue dots) in general characterize the phase retardance effect. The lower values of these elements are characteristics of phase randomization leading to a lower value of the retardance parameter. The first row and first column of the Mueller matrix (shown with a green box) primarily encodes the diattenuation property of the medium. The lower value of these elements represents lower magnitude of diattenuation, signifying random organization/orientation effects. In order to quantify these effects, the Mueller matrices were decomposed. The decomposition derived parameters are shown in Figure 3C–E. As anticipated, the decomposition yielded significant magnitudes of linear retardance. The dependence of the individual parameters on the phase transition behavior is described subsequently. Once the competence of MMP to examine the phase separation behavior was observed, we then executed the cloud point analysis. The plateau observed at 600 nm in most cases motivated us to choose parameter values at that particular wavelength for the quantification of cloud points (Figure 3C–E).

The phase separation behavior evaluated from the individual parameters enlightened us to the activities of SRPs in aqueous medium (Figures 4 and S2–S4). Initially, we focused on the macroscopic parameter, depolarization (Δ). The Δ value predominantly originates from (i) multiple scattering effects within the sample and (ii) randomly oriented spatial domains of birefringent structures.[17] Since depolarization is a bulk property, the phenomenon of CICPS was evident from the cloud point analysis by means of Δ values at 600 nm. The strong multiple scattering effects escalated the turbidity of the solution and resulted in an increased Δ value upon hydrophilic to hydrophobic switch over (Figures 4A, S2A, S3A, and S4A).

DOI: 10.1021/acs.analchem.5b01794
Anal. Chem. XXXX, XXX, XXX−XXX

Above a solution concentration of 0.25 mg/mL, a stagnancy in the shift of cloud points determined from Δ values was observed.

The magnitude of the second MMP derived parameter diattenuation depends on (i) anisotropic absorption from oriented/organized structure and (ii) scattering, reflection/transmission of light through layered structures.[17] The gradient directionality of d value-derived sigmoidal curve of the phase separation behavior was significantly influenced by the choice of external stimuli. In the case of thermoresponsive polymers, the d value increased when polymer lost its hydrophilicity (Figures 4B and S3B). In contrast, the pH responsive polymers, once becoming hydrophobic, showed a drop in d value (Figures S2B and S4B). The increased d value is a consequence of orientational anisotropy at microdomains. The unusual behavior manifested as a sigmoidal pH dependent diattenuation possibly originates from the loss of anisotropy due to the introduction of novel polarizable groups for tuning solution pH. However, this mechanism is still not very well understood. Apart from the unresolved sigmoidal behavior mentioned above, we were able to determine hydration polarity change at ∼1.1−1.4 μM polymer concentration (0.01 mg/mL) with only ∼5.0−10 μL of solution. Note that such polymer economic methodology has never been reported before through any experimental techniques.

The inquisitiveness regarding the CICPS was resolved from analyzing phase change behavior via linear retardance parameter δ. The linear retardance effect originates from the organization of discrete anisotropic domains. The net value of δ is determined by several factors such as the magnitude of (anisotropic) polarizability and the homogeneity in molecular structure.[17,32] It is worth mentioning that the dominance in randomness of the system can substantially diminish the δ value. For example, when PNIPAM is in aqueous medium below its LCST, the polymer molecules are hydrophilically hydrated. In that case, the extended water−water hydrogen bonding is destructed for solvating PNIPAM by means of co-operative polymer−water hydrogen bonding. Once the LCST is reached, the PNIPAM molecules in water become hydrophobically hydrated. Where the PNIPAM−water hydrogen bonding interaction (hydration shell) is broken and water retains its original co-ordination state,[33] the entropy of hydrophilic hydration is more when compared to that of hydrophobic hydration.[33,34] The increase in linear retardance of PNIPAM and its copolymer solution after LCST appears to originate predominantly from this entropy change occurring through disruption of polymer−water hydrogen bonds (Figures 4C and S3C).The later stage is the accumulation of hydrophobic polymers via hydrogen bonding (polymer−polymer). Probing transition point by means of linear retardance interestingly did not show CICPS (Figures 4C and S2C). The diminished CICPS is presumed to be occurring because of the direct relation of linear retardance with randomness.[17,19,20]

The typical diminishing of CICPS in transition points determined from d and δ values of PNIPAM thus provided information on the first step of cloud point generation (hydrogen bonding breakage) which is independent of concentration.[12] Similar trends were observed in the case of pH responsive homo- and copolymers as well (Figures S2C and S4C). The cloud point assessed from transmittance, Δ, d, and δ values of homo- and copolymers is summarized in Figure 5 and Tables S2 and S3. The results clearly demonstrate the novel ability of the MMP derived polarization parameters in probing/quantifying both macro- and microscopical phenomena of phase separation.

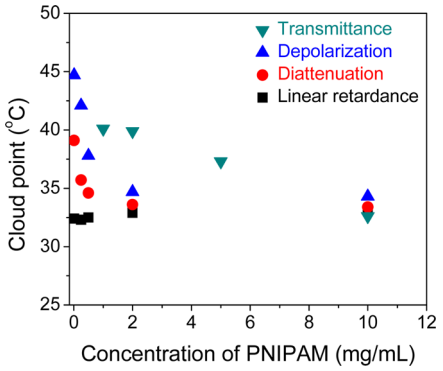

Figure 5. Summary of cloud point assessed with transmittance and various Mueller matrix derived parameters of PNIPAM.

CONCLUSIONS

In summary, MMP allowed us to monitor both macro- and microscopic visualization of the cloud point generation phenomenon by SRPs in the presence of external stimuli. The cloud points assessed from depolarization Δ values were found to be dependent on polymer concentration while diattenuation d (mostly) and linear retardance δ derived cloud points were independent of polymer concentration in aqueous medium. The combination of Δ, d, and δ parameters derived from inverse analysis with polar decomposition of the Mueller matrix provided unique information regarding phase separation behavior economically. A few hundred times lower concentration was only required for judging the phase behavior in contrast to the present technology. For PNIPAM solutions (at various concentrations), the cloud point observed via transmittance (37.48 ± 5.97) and depolarization (38.72 ± 9.15) had higher deviation when compared to the diattenuation (35.28 ± 4.65) and linear retardance (32.64 ± 0.69) derived cloud points. In addition, no single technique so far has been developed which can essentially provide the information concerning the two step behavior of cloud point generation that we obtained through MMP.

ASSOCIATED CONTENT

Supporting Information

The Supporting Information is available free of charge on the ACS Publications website at DOI: 10.1021/acs.analchem.5b01794.

Details of materials, additional figures, and tables as noted in the main text (PDF)

AUTHOR INFORMATION

Corresponding Authors

*E-mail: p_de@iiserkol.ac.in (P.D.).
*E-mail: nghosh@iiserkol.ac.in (N.G.).

Notes

The authors declare no competing financial interest.

ACKNOWLEDGMENTS

A N. acknowledges Department of Science and Technology (DST), India for the INSPIRE-SHE scholarship.

DOI: 10.1021/acs.analchem.5b01794
Anal. Chem. XXXX, XXX, XXX−XXX

REFERENCES

(1) Nath, N.; Chilkoti, A. *Adv. Mater.* **2002**, *14*, 1243−1247.
(2) Cohen Stuart, M. A.; et al. *Nat. Mater.* **2010**, *9*, 101−113.
(3) Uhlig, K.; Boysen, B.; Lankenau, A.; Jaeger, M.; Wischerhoff, E.; Lutz, J.-F.; Laschewsky, A.; Duschl, C. *Biomicrofluidics* **2012**, *6*, 024129.
(4) Pietsch, C.; Hoogenboom, R.; Schubert, U. S. *Angew. Chem., Int. Ed.* **2009**, *48*, 5653−5656.
(5) Chang, C.-W.; Nguyen, T. H.; Maynard, H. D. *Macromol. Rapid Commun.* **2010**, *31*, 1691−1695.
(6) Li, M.; Li, H.; De, P.; Sumerlin, B. S. *Macromol. Rapid Commun.* **2011**, *32*, 354−359.
(7) Li, H.; Li, M.; Yu, X.; Bapat, A. P.; Sumerlin, B. S. *Polym. Chem.* **2011**, *2*, 1531−1535.
(8) Byeon, J. H.; Kim, J.-W. *ACS Macro Lett.* **2014**, *3*, 369−372.
(9) Zayas, H. A.; Lu, A.; Valade, D.; Amir, F.; Jia, Z.; O'Reilly, R. K.; Monteiro, M. J. *ACS Macro Lett.* **2013**, *2*, 327−331.
(10) Rowe, M. D.; Chang, C.-C.; Thamm, D. H.; Kraft, S. L.; Harmon, J. F., Jr.; Vogt, A. P.; Sumerlin, B. S.; Boyes, S. G. *Langmuir* **2009**, *25*, 9487−9499.
(11) Bebis, K.; Jones, M. W.; Haddleton, D. M.; Gibson, M. I. *Polym. Chem.* **2011**, *2*, 975−982.
(12) Boutris, C.; Chatzi, E. G.; Kiparissides, C. *Polymer* **1997**, *38*, 2567−2570.
(13) Pietsch, C.; Schubert, U. S.; Hoogenboom, R. *Chem. Commun.* **2011**, *47*, 8750−8765.
(14) (a) Seuring, J.; Agarwal, S. *Macromol. Rapid Commun.* **2012**, *33*, 1898−1920. (b) Zhang, Q.; Vancoillie, G.; Mees, M. A.; Hoogenboom, R. *Polym. Chem.* **2015**, *6*, 2396−2400. (c) Narayanan, A.; Bauri, K.; Ruidas, B.; Pradhan, G.; Banerjee, S.; De, P. *Langmuir* **2014**, *30*, 13430−13437.
(15) De, P.; Sumerlin, B. S. *Macromol. Chem. Phys.* **2013**, *214*, 272−279.
(16) Wolff, M.; Braun, D.; Nash, M. A. *Anal. Chem.* **2014**, *86*, 6797−6803.
(17) Ghosh, N.; Vitkin, A. I. *J. Biomed. Opt.* **2011**, *16*, 110801.
(18) Lu, Y. S.; Chipman, R. A. *J. Opt. Soc. Am. A* **1996**, *13*, 1106−1113.
(19) Patil, N.; Soni, J.; Ghosh, N.; De, P. *J. Phys. Chem. B* **2012**, *116*, 13913−13921.
(20) Patil, N.; Roy, S. G.; Haldar, U.; De, P. *J. Phys. Chem. B* **2013**, *117*, 16292−16302.
(21) Hall, S. A.; Hoyle, M.-A.; Post, J. S.; Hore, D. K. *Anal. Chem.* **2013**, *85*, 7613−7619.
(22) (a) Roy, S. G.; Bauri, K.; Pal, S.; Goswami, A.; Madras, G.; De, P. *Polym. Int.* **2013**, *62*, 463−473. (b) Bauri, K.; Roy, S. G.; Arora, S.; Dey, R. K.; Goswami, A.; Madras, G.; De, P. *J. Therm. Anal. Calorim.* **2013**, *111*, 753−761.
(23) Moad, G.; Rizzardo, E.; Thang, S. H. *Aust. J. Chem.* **2005**, *58*, 379−410.
(24) Dan, K.; Ghosh, S. *Polym. Chem.* **2014**, *5*, 3901−3909.
(25) Willcock, H.; Lu, A.; Hansell, C. F.; Chapman, E.; Collins, I. R.; O'Reilly, R. K. *Polym. Chem.* **2014**, *5*, 1023−1030.
(26) (a) Xia, Y.; Yin, X.; Burke, N. A. D.; Stover, H. D. H. *Macromolecules* **2005**, *38*, 5937−5943. (b) Lutz, J.-F.; Akdemir, O.; Hoth, A. *J. Am. Chem. Soc.* **2006**, *128*, 13046−13047. (c) Hoogenboom, R.; Thijs, H. M. L.; Jochems, M. J. H. C.; van Lankvelt, B. M.; Fijten, M. W. M.; Schubert, U. S. *Chem. Commun.* **2008**, 5758−5760.
(27) Roy, D.; Brooks, W. L. A.; Sumerlin, B. S. *Chem. Soc. Rev.* **2013**, *42*, 7214−7243.
(28) Sanchez, I. C.; Stone, M. *Polymer Blends*; Paul, D. R., Bucknall, C. B., Eds.; John Wiley & Sons, Inc.: New York, 2000; Vol. *1*, p 51.
(29) (a) De Martino, A.; Garcia-Caurel, E.; Laude, B.; Drévillon, B. *Thin Solid Films* **2004**, *455-456*, 112−119. (b) Stabo-Eeg, F. Development of instrumentation for Mueller matrix ellipsometry. PhD Dissertation, Norwegian University of Science and Technology, 2009.
(30) Soni, J.; Purwar, H.; Lakhotia, H.; Chandel, S.; Banerjee, C.; Kumar, U.; Ghosh, N. *Opt. Express* **2013**, *21*, 15475−15489.
(31) Ghosh, N.; Wood, M.; Vitkin, A. I. In *Handbook of Photonics for Biomedical Science*; Valery, V. T., Ed.; Taylor and Francis Publishing: Boca Raton, FL, 2010; Chapter 9.
(32) Chipman, R. A. In *Handbook of Optics*, 2nd ed.; Bass, M., Ed.; McGraw-Hill: New York, 1994; Vol. *2*, Chapter 22, pp 22.1.
(33) Collins, K. D. *Proc. Natl. Acad. Sci. U. S. A.* **1995**, *92*, 5553−5557.
(34) Nemethy, G.; Scheraga, H. A. *J. Chem. Phys.* **1962**, *36*, 3382−3400.

DOI: 10.1021/acs.analchem.5b01794
Anal. Chem. XXXX, XXX, XXX−XXX